JOURNAL OF MATERIALS SCIENCE **40** (2005) 2411 – 2416

# Observations of the advancing $\delta$-ferrite/$\gamma$-austenite/liquid interface during the peritectic reaction

N.J. MCDONALD, S. SRIDHAR*
*Department of Materials Science and Engineering, Carnegie Mellon University, 5000 Forbes Ave., Pittsburgh, PA, 15213, USA*
*E-mail: sridhars@andrew.cmu.edu*

The peritectic transition, where $\delta$-ferrite and liquid transform into $\gamma$-austenite, is an important aspect of product quality and process control in many ferrous and non-ferrous alloys. Due to the high temperatures at which the transition takes place, relatively little experimental work has been carried out to quantify the underlying phenomena. This paper presents recent work in visualizing the peritectic reaction stage of the transition. The visualization was carried out on the surface of hyperperitectic Fe-4.7 wt% Ni samples using a Confocal Scanning Laser Microscope (CSLM) equipped with a gold-image furnace. The focus of the research is to quantify the rate and shape evolution of the $\gamma$-austenite phase as it envelopes the $\delta$-ferrite grains. Tip radii of 8 and 5 $\mu$m were witnessed and it was found that, as these tips approached one-another their shape was altered and their growth rates decreased due to soft impingement of their respective diffusion fields. Comparing the separation distance at the point of soft impingement with the tip radius suggested a proportionality constant between tip radius of curvature and diffusion field size of between 1.1 and 1.3. 

## 1. Introduction

The peritectic transition is a topic of importance in modern casting due to the defects which have been attributed to it. The volume change associated with the transition from $\delta$-ferrite and liquid to austenite, Equation 1, causes the casting to pull away from the mould, leading to a decrease in heat flux which, in turn, leads to thin spots. These thin areas on the surface of the casting then have a higher chance of cracking, deforming, or causing a breakout [1–3]. Other relations between the peritectic reaction and surface defects are that longitudinal face cracks on the surface of cast steels have been associated with the fraction of ferrite and austenite [4] and that both longitudinal as well as transverse facial cracking are related to austenite grain formation [5]. It should be noted that a peritectic transition is witnessed in a broad range of materials, including ferrous, copper, and aluminum alloys as well as magnetic and electronic materials.

$$\delta + L \rightarrow \gamma \tag{1}$$

A description of the mechanism of the peritectic transition has been given by numerous authors [6–12]. Kerr *et al.* [7] split the transition into three distinct regimes: reaction, transformation, and solidification. The peritectic reaction requires that all three phases be in contact with one another during the growth of $\gamma$ and it is this stage which will be the focus of the present work, specifically, the shape of the $\gamma$ phase enveloping the $\delta$-front will be investigated.

Early theories of the peritectic reaction [6] were based on the equilibrium phase diagram, as shown in Fig. 1. More detailed theories [7–11] state that at some temperature below the ferrite liquidus and above the peritectic temperature, properitectic $\delta$-ferrite will form. Then, at a certain undercooling below the peritectic temperature, austenite will begin to form along the ferrite/liquid boundary and divide these two phases. Some experimental evidence to this effect is given by St. John and Hogan [13] who observed that, although Reaction (1) would suggest an isothermal reaction, a thermal arrest is either very short or not witnessed during continuous cooling experiments. This might suggest that Reaction (1) does not go to completion and that, instead, the austenite envelope forms around the $\delta$-ferrite. The $\gamma$ phase can envelope the $\delta$ phase very quickly because the liquid in equilibrium with austenite is supersaturated with respect to the solute due to the undercooling being applied.

In order to quantitatively describe the rate of the advancing austenite phase across the ferrite/liquid boundary, a number of models have been reported [14–18]. The simplest of these begins with Fick's 1st Law and combines it with a mass balance in order to give an

*Author to whom all correspondence should be addressed.

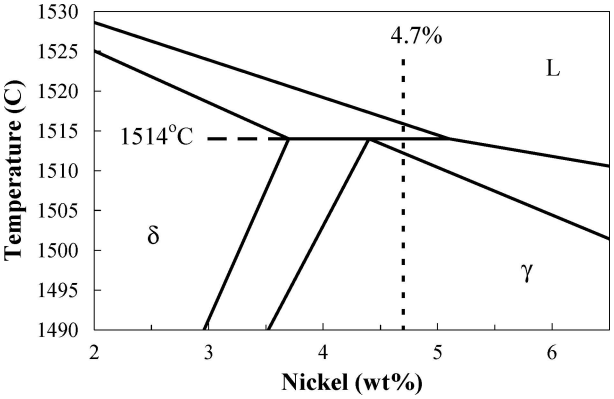


*Figure 1* Peritectic region of the iron-nickel phase diagram.

equation for the velocity of the austenite/liquid boundary as a function of the diffusion coefficient, the concentration of the two phases, and the concentration gradient in the parent phase ahead of the moving interface. Zener [15], while studying the kinetics of austenite decomposition, elaborated on this model by assuming that the diffusion profile of the parent phase is steady-state and that there is no diffusion in the growing phase and developed Equation 2.

$$V_B = \frac{\Delta C_0}{(C_2 - C_1)}(D/L) \tag{2}$$

where $V_B$ is the velocity of the boundary, $\Delta C_0$ is the concentration difference between the two phases, $C$ is the number of solute atoms per unit volume, $D$ is the the interdiffusion coefficient, $L$ is the thickness of the boundary layer, and the subscripts refer to the phases.

Performing a mass balance on the solute gives a relationship between the diffusion distance and the position of the solid/liquid interface relative to is starting location. If this interface is convex towards the parent phase, however, then the diffusion distance would be proportional to the radius of curvature of the growing phase and there must be some minimum radius that would give a maximum growth rate for the growing austenite. This radius can be determined because, due to Gibbs-Thomson effect, the driving force for diffusion will be a function of tip radius and there will be some critical radius, $r_c$, at which there is no concentration difference to drive diffusion. This argument leads to a modified relationship between the velocity of the moving boundary and the diffusion distance, Equation 3.

$$V_B = \frac{\Delta C_0}{(C_2 - C_1)}\left(\frac{D}{ar}\right)\left(1 - \frac{r_c}{r}\right) \tag{3}$$

where $a$ is the proportionality constant between that relates the boundary layer thickness, $L$, and tip radius, $r$.

Hillert [16] modified this model by beginning with the partial differential equation of Fick's 2nd Law, and solving it using the method of separation of variables. He assumes no diffusion in the new phase and uses the change in composition along the front with the effect of curvature included as a boundary condition. Using this approach, Hillert finds an equation analogous to Equation 3 and derives that the proportionality constant, $a$, must have a value of 2 to be in agreement with Zener's model.

Numerous researchers have used the models' of Zener [15] and Hillert [16] in order to predict or explain results for austenite decomposition, peritectic reaction, and other proposed or assumed diffusion-controlled processes [16, 19–24]. Experimental verification of the predictions of peritectic phenomena has been limited due to the high temperature at which they occur. Also, subsequent phase transformations at lower temperatures make it difficult to draw conclusions from microstructures of quenched samples.

The possibility of using a Confocal Scanning Laser Microscope (CSLM) to carry out solidification experiments has been shown recently by a number of researchers [23–26]. Previous work has utilized this tool to measure the rate of austenite formation in peritectic systems and has found that the growing phase moves at a constant rate across the ferrite/liquid boundary and that this rate increases with the driving force provided to the reaction [24]. The objective of the present work is to use the CSLM to observe, *in-situ*, the interaction of the diffusion fields of growing austenite phases as they approach one another along the solid/liquid interface. From these observations a comparison of the relationship between radius and diffusion distance will be developed and compared against the theoretical prediction of Hillert [16].

## 2. Materials, equipment, and procedure

### 2.1. Materials

The iron-nickel system, as shown in Fig. 1, displays peritectic attributes between 3.7 to 5.1 wt% nickel with a peritectic invariant at 4.4 wt%. An alloy containing 4.7 wt% nickel was prepared in an induction furnace using iron pieces (99.97+%) and nickel shot (99.95+%). This composition was chosen to represent the hyperperitectic case. Samples for the CSLM experiments were taken using a quartz tube while the master alloys were molten and then cut into the appropriate size.

### 2.2. High temperature confocal scanning laser microscope

The Confocal Scanning Laser Microscope 1LM21H equipped with a gold image hot-stage, is a tool for observing high temperature phenomena *in-situ* under controlled thermal fields and gas atmospheres. It has been described in detail in the literature previously [27, 28] and uses a He-Ne laser beam (1.5 mW, 632.8 nm) to two-dimensionally scan the surface of a solid or molten material. The deflected beam is then passed through a pinhole on its way to a light sensor whose signals are then displayed on a television screen and can be recorded by VCR or sent to a computer for future analysis. Images can be captured at a rate of thirty frames per second. High contrast systems can be viewed and high resolution achieved due to the set-up of the objective lenses and associated apparatus.

The sample itself is placed in a high purity alumina ($Al_2O_3$) cylindrical crucible that has dimensions

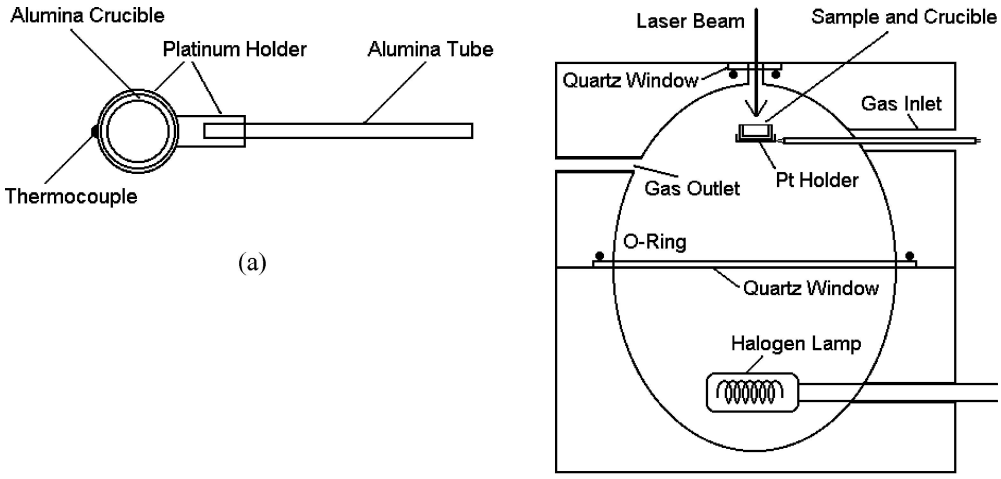


*Figure 2* (a) Schematic of alumina crucible and platinum holder (b) Interior of gold-plated image furnace including crucible and holder.

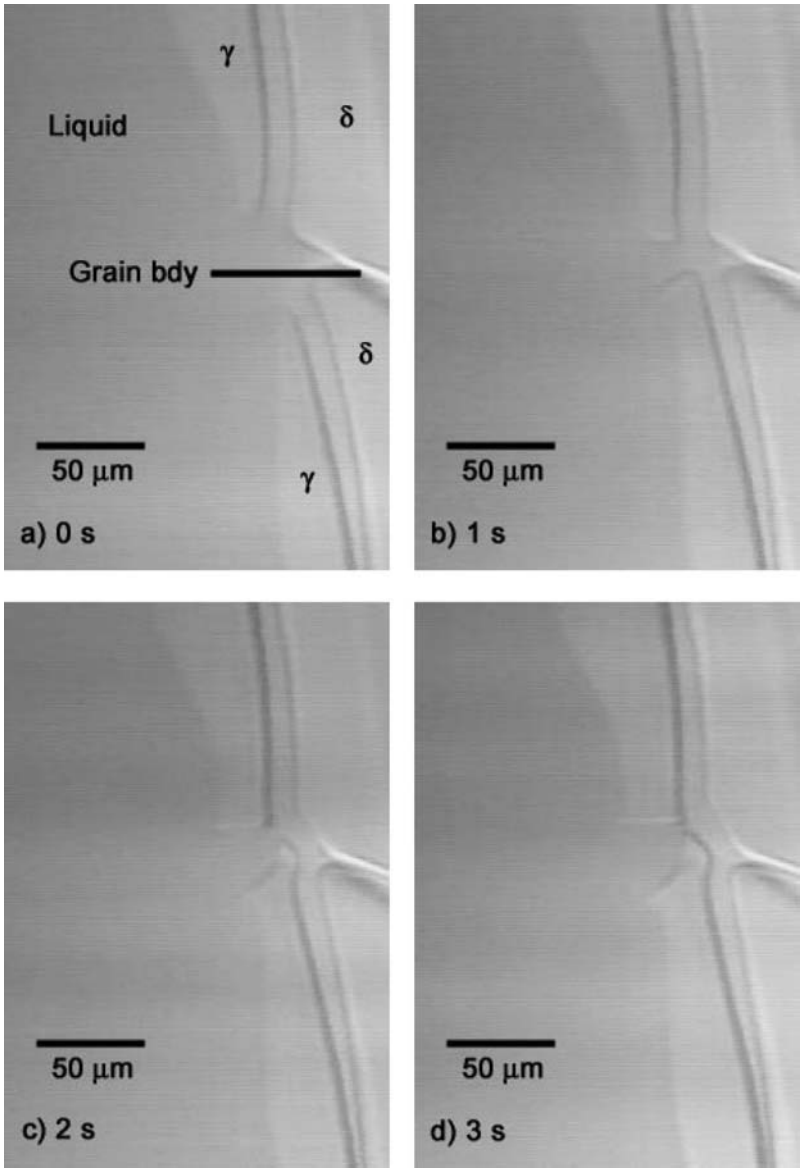


*Figure 3* Austenite fields approaching one another at 1°C undercooling for Fe-4.7 wt% Ni system.

of 5.5 mm O.D. × 3 mm I.D. × 3 mm height. This crucible is then rested on a platinum pan wired with one Pt-6%Rh/Pt-30%Rh thermocouple as shown in Fig. 2a. In the image furnace, shown as Fig. 2b, a halogen lamp at the bottom provides heat to the sample. The laser beam enters through a port that is covered airtight by a quartz plate and o-ring. A wide range of atmospheres can be maintained in the furnace through a gas inlet and vacuum pump.

### 2.3. Procedure

The procedure used to carry out peritectic solidification experiments and the operational conditions of the furnace have been outlined in detail by the authors elsewhere [24]. The atmosphere in the furnace was controlled through a cycle of vacuum pumping followed by purging the furnace with high purity Ar gas (99.996%) to lower the oxygen partial pressure. The temperature distribution in the furnace was found to be even within 1.5 mm of the focal point and then to decrease roughly linearly on either side at a gradient of 4 K/mm.

The experiment itself consisted of growing planar delta-ferrite, holding the ferrite/liquid boundary at or just above the peritectic temperature and subsequently dropping the temperature rapidly by a predetermined amount. The melt was maintained at the undercooled temperature for the duration of the observations. Experiments on pure Fe samples showed, as would be expected, that no growth along the solid/liquid interface occurred, only planar movement toward the melt.

At large undercoolings some solid grew directly out of the liquid ahead of the solid/melt interface, thus hindering any attempt to accurately measure the reaction rate. This growth may occur because the bulk melt is experiencing a greater driving force than the solid/liquid interface.

## 3. Results and discussion

The peritectic reaction was recorded at undercooling temperatures between 1 and 4°C. It should be stressed that the melt itself is isothermal near the solid/melt interface (where the peritectic reaction occurs) due to the size of the growing austenite field compared to the

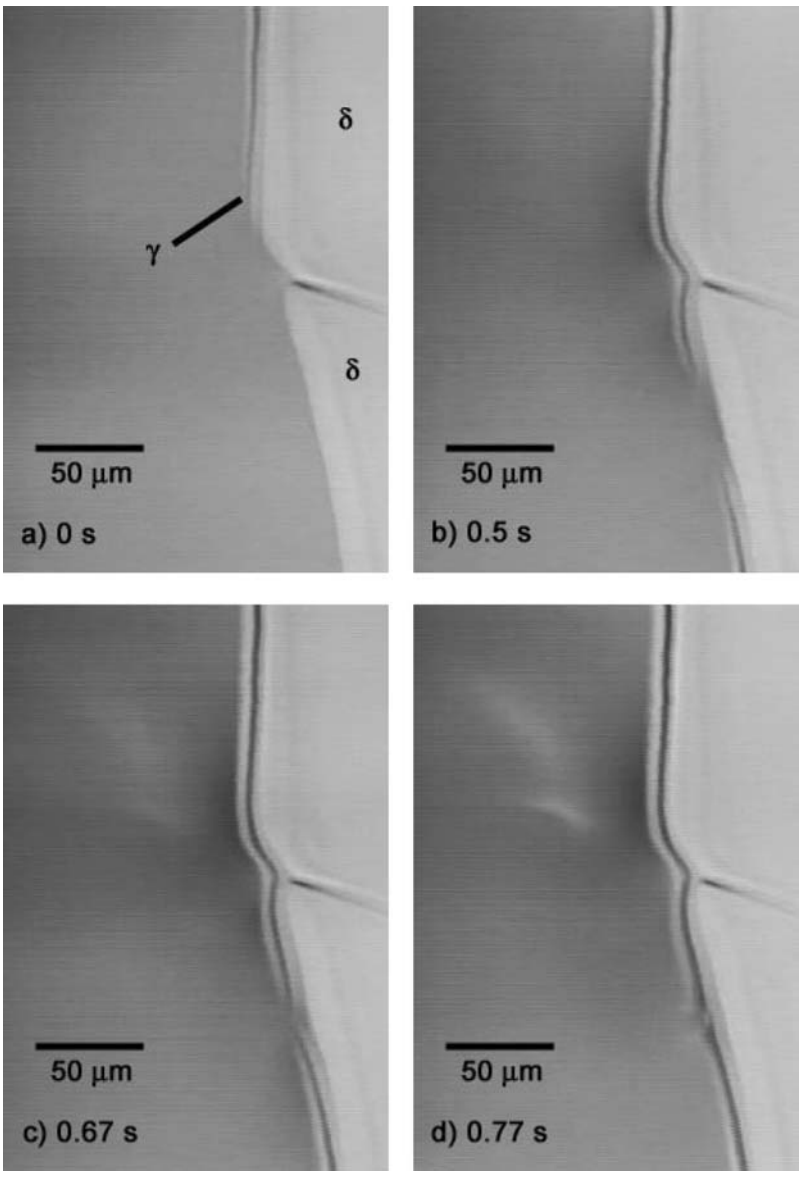


*Figure 4* Austenite fields approaching one another at 4°C undercooling for Fe-4.7 wt% Ni system.

temperature gradient discussed earlier. The undercooling ($\Delta T_{\text{under}}$) refers to the temperature below the peritectic temperature. This is the driving force for the reaction stage.

Figs 3 and 4 show the progression of austenite along the ferrite/liquid boundary at undercoolings of 1 and 4°C, respectively, for the Fe-4.7 wt% Ni system. All phases present are labeled in Figs. 3a and 4a. The main difference between the cases shown are the tip radius of the growing austenite fields which are 8 $\mu$m for the 1°C case and 5 $\mu$m for an undercooling of 4°C. Results similar to that of the 4°C case were observed at 2 and 3°C below the peritectic temperature also.

While the growing tips remained far from one another, it was observed that the growing austenite phase moved at a constant rate which was proportional to the undercooling. This rate is given by Equation 4 and matches the prediction of increased rate with increased undercooling given by the model of Bosze-Trivedi [18] over the experimental range of undercoolings [24].

$$V = (30.3\Delta T_{\text{under}} - 16.1) \pm 3.2\ \mu\text{m/s} \qquad (4)$$

where $V$ is the growth rate in $\mu$m/s and $\Delta T_{\text{under}}$ is the driving force provided to the reaction, given by the difference between the experimental temperature and the peritectic temperature.

The shape of the three-phase $\delta/\gamma$/liquid junction and the tip radius and shape did not vary significantly during the period where the distance between tips was large and the velocity constant.

As the two growing phases become close there is a deformation evident and the tips become flatter, as shown in Figs 3b and 4d. Also, the velocity of the moving $\delta/\gamma/L$ junction decreases dramatically, as shown in Fig. 5, which seems to suggest that this is the point at which the diffusion fields have begun to overlap. Fig. 5 also shows the distance of the two tips from one another and from this information one can ascertain the relationship between radius of curvature and diffusion length. Another interesting observation is that, most clearly for the 1°C case but also for 2 and 3°C of undercooling, there is a sudden movement in the position of the interface at approximately 2 s and a corresponding drop in the distance between the two tips. This can be explained by an abrupt deformation in the shape of the growing austenite, as seen in Fig. 3c. Deformation of the same magnitude was not witnessed for the 2, 3, or 4°C cases, but this may be due to the smaller radii of curvature and the faster growth rates in these instances.

There are, thus, three regimes witnessed for the growth of austenite along the ferrite/liquid interface. Regime I is the constant velocity and radius of curvature that is seen while the austenite phases are far away from each other, Regime II is the decrease in velocity as the diffusion fields overlap, and Regime III occurs due to sudden deformation as the growing austenite tips respond to the interference of the two diffusion fields.

The decrease in velocity of the growing austenite corresponds to a distance of 18 $\mu$m for the 1°C case and 13 $\mu$m for the 4°C case as shown in Fig. 5a and 5b, respectively. Since there are two austenite tips and, hence, two diffusion fields, the diffusion length for each tip is one-half of the measured distance. Therefore, the size of the diffusion field for a tip radius of 8 $\mu$m is 9 $\mu$m and is 6.5 $\mu$m for a tip radius of 5 $\mu$m. This would give the proportionality constant (L/r) values of 1.1 and 1.3 respectively.

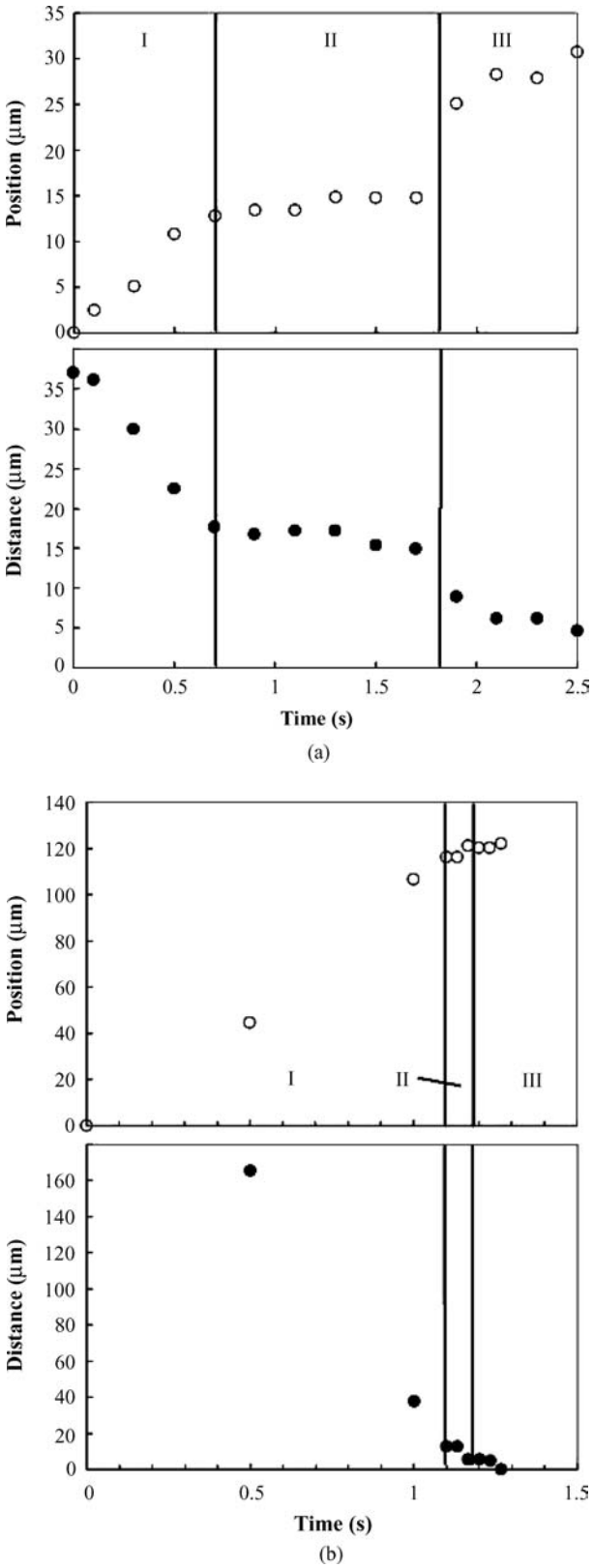


*Figure 5* Position of $\delta/\gamma$/L junction and distance of austenite tips from one another for (a) 1°C undercooling and (b) 4°C undercooling for Fe-4.7 wt% Ni system.

As discussed in the Introduction, Hillert [16] predicted a value of 2 for this constant by developing an expression analogous to Equation 3. Therefore, although the general trend is in line with the predictions of Hillert, there is a slight difference between the observed and predicted values which may come from a number of different sources. First, Hillert [16] and Zener [15] developed their models based on an assumption of maximum growth. It is possible that the austenite observed was not growing at maximum rate, however, this is unlikely due to the constant rate and reasonable agreement between observation and model shown previously [24]. Also, since the CSLM is inherently a surface technique, there is the potential for fluid flow and for the system to not be at complete equilibrium due to the temperature gradients measured. This could have an impact on diffusion distance by creating a more completely stirred system at the moving austenite/liquid boundary. Whatever the explanation, the observation of diffusion distance and its relationship to radius of curvature is important for the further development of models to predict the rate of peritectic reaction and to compare this prediction against experimental results in the CSLM.

## 4. Conclusions

The progression of austenite along the $\delta$-ferrite/liquid boundary has been observed and its rate and shape evolution analyzed using a Confocal Scanning Laser Microscope. For the Fe-4.7 wt% Ni system austenite tip radii of 8 and 5 $\mu$m were witnessed and it was found that there are three distinct regimes of growth of the $\gamma$-austenite front. The first is that the growing phase advanced at a rate that was proportional to undercooling and that its tip shape remained constant when adjacent approaching fronts were sufficiently far apart. The second regime was that, as the austenite tips approached one-another, their shapes were altered and their growth rates decreased due to soft impingement by diffusion fields. Comparing the separation distance at the point of tip shape change with the tip radius suggested a proportionality constant between tip radius of curvature and diffusion field size of between 1.1 and 1.3. The final regime of growth was a sudden deformation of the growing tip due to the interference of the two diffusion fields with one another.

## References


1. S. N. SINGH and K. E. BLAZEK, *J. Metals* **26** (1974) 17.
2. M. SUZUKI and Y. YAMAOKA, *Mater. Trans.* **44** (2003) 836.
3. E. T. TURKDOGAN, "Fundamentals of Steelmaking" (UK, The Institute of Materials, London, 1996) p. 104.
4. Y. K. CHUANG, D. REINISCH and K. SCHWERDTFEGER, *Metall Trans. A* **6A** (1975) 235.
5. A. W. CRAMB, (ed.), "The Making Shaping and Treating of Steel: Casting Volume, 11th ed.," (AISE Steel Foundation, Pittsburgh, PA, 2003).
6. J. A. SARTELL and D. J. MACK, *J. Inst. Metals* **93** (1964-65) 19.
7. H. W. KERR, J. CISSÉ and G. F. BOLLING, *Acta Met.* **22** (1974) 677.
8. M. HILLERT, "Solidification and Casting of Metals" (The Metals Society, London, UK, 1979) p. 81.
9. H. FREDRIKSSON, *Met. Sci.* **10** (1976) 77.
10. D. H. ST. JOHN, *Acta Metall. Mater.* **38** (1990) 631.
11. Y. K. CHUANG, D. REINISCH and K. SCHWERDTFEGER, *Metall Trans A* **6A** (1975) 235.
12. H. FREDRIKSSON and J. STJERNDAHL, *Met. Sci.* **16** (1982) 575.
13. D. H. ST. JOHN and L. M. HOGAN, *J. Mater. Sci.* **17** (1982) 2413.
14. D. A. PORTER and K. E. EASTERLING, "Phase Transformations in Metals and Alloys" (Chapman and Hall, New York, USA, 1992).
15. C. ZENER, *Trans. AIME* **167** (1946) 550.
16. M. HILLERT, *Jernkont. Ann.* **141** (1957) 757.
17. R. TRIVEDI, *Acta Metall.* **18** (1970) 287.
18. W. P. BOSZE and R. TRIVEDI, *Metall. Trans.* **5** (1974) 511.
19. C. ATKINSON, H. B. AARON, K. R. KINSMAN and H. I. AARONSON, *Metall. Trans.* **4** (1973) 783.
20. R. G. KAMAR, E. B. HAWBOLT, L. C. BROWNE and J. K. BRIMACOMBE, *Metall. Trans. A* **23** (1992) 2469.
21. F. FAZELI and M. MILITZER, *Steel Res.* **73** (2002) 242.
22. H. FREDRIKSSON and T. NYLEN, *Met. Sci.* **16** (1982) 283.
23. H. SHIBATA, Y. ARAI, M. SUZUKI and T. EMI, *Metall Mat. Trans. B* **31B** (2000) 981.
24. N. J. McDONALD and S. SRIDHAR, *Metall. Mat. Trans. A* **34A** (2003) 1931.
25. Y. WANG, M. VALDEZ and S. SRIDHAR, *Metall. Trans. B* **33B** (2002) 625.
26. Y. WANG, M. VALDEZ and S. SRIDHAR, *Z. Metallkunde* **93** (2002) 12.
27. H. SHIBATA, T. EMI and M. SUZUKI, *Mater. Trans. JIM* **37** (1996) 620.
28. A. W. CRAMB, C. ORRLING, Y. FANG, N. PHINICHKA and S. SRIDHAR, *JOM* **51** (1999) 11.


*Received 31 March*
*and accepted 18 July 2004*